Nanomechanical Device

A Two-State DNA Lattice Switched by DNA Nanoactuator**

*Liping Feng, Sung Ha Park, John H. Reif, and Hao Yan**

Controlled mechanical movement in molecular scale devices is one of the key goals of nanotechnology. DNA is an excellent candidate for the construction of such devices due to the specificity of base pairing and its robust physicochemical properties. Well-known as the genetic material, DNA has recently been explored as a smart material for constructing periodically patterned structures[1–3] and nanomechanical devices.[4–8] A variety of DNA-based molecular machines[9] displaying rotational[4,6] and open/close movements[5,7,8] have recently been demonstrated. Reversible shifting of the equilibrium between two conformational states is triggered by changes in external conditions or by the addition of a "DNA fuel strand" that provides the driving force for such changes. Incorporation of DNA devices into arrays could lead to complex structural states suitable for nanorobotic applications if each individual device can be addressed separately. Yan et al.[6] have recently demonstrated a linear one-dimensional DNA array displaying a switch of *cis* and *trans* conformations through the rotational motion of a robust sequence-dependent DNA nanodevice. In the further exploration of the potential applications of DNA-based molecule machines in nanorobotics, a major challenge is to implement molecular machines into two-dimensional (2D) or three-dimensional (3D) patterned arrays. This has numerous potential applications. 1) The size and shape of the lattice could be programmed through the control of sequence-dependent devices, leading to controlled nanofabrication of molecular nanoelectronic wires with "on" and "off" states. For example, the tunneling effect of quantum-dot cellular automata could be actuated by controlling the distance between adjacent cells. 2) Molecules or nanoparticles could be selectively manipulated, for example, sorted and transported, by using molecular motor devices arranged on DNA

[*] Prof. Dr. H. Yan, L. Feng, Prof. Dr. J. H. Reif
Department of Computer Science
Duke University
Durham, NC 27708 (USA)
Fax: (+1) 919-660-6519
E-mail: hy1@cs.duke.edu
S. H. Park
Department of Physics
Duke University
Durham, NC 27708 (USA)

[**] We thank Prof. Erik Winfree for helpful discussions on using mismatched base pairs in the nanoactuator device. We also thank Dr. Yan Liu for assistance with the FRET measurements. This work has been supported by grants from the NSF to H.Y. (EIA-0218359) and to J.H.R. (EIA-00-86015), and from DARPA/AFSOR (F30602-01-2-0561) to J.H.R.

Supporting information for this article is available on the WWW under http://www.angewandte.org or from the author.

  DOI: 10.1002/anie.200351818

tiling arrays, which may lead to programmed chemical synthesis. 3) It may offer a mechanism for DNA computation of arrays whose elements (the tiles) hold state.

Herein we report the construction of a robust sequence-dependent DNA device, which we call a nanoactuator, and the incorporation of such a device into a 2D parallelogram DNA lattice. Figure 1 illustrates the design and the operation of the nanoactuator device. The two states of the device are shown as S1 and S2. S1 consists four strands assembled through Watson–Crick base pairing to form a bulged three-arm DNA branch-junction. Leontis and colleagues[11] have previously shown that a three-arm DNA branch-junction containing a loop of two deoxythymidine nucleotides has a preferred stacking direction. Bulged three-arm DNA branch-junctions have been well characterized by Liu et al.[13] and have been extensively used in DNA nanoconstruction[14,15] and as topographic markers in the self-assembly of 2D DNA lattices.[1,2] Thus, a DNA device based on a bulged three-arm junction is an excellent candidate to serve as actuator for DNA lattices. The stem-loop joining the two strands of the duplex contains 21 nucleotides and is composed of a loop of two deoxythymidine nucleotides, a seven-base-pair duplex region (contains two mismatched pairs), and a loop of five deoxythymidine nucleotides. In Figure 1 the strand in red is a set strand (SS1) that sets the nanoactuator device in the S1 state. S2 consists of the same three black strands as in S1, but a blue strand (SS2), which has a region fully complementary to the stem-loop sequence, replaces the red strand. SS2 serves to open up the stem-loop in S1 and set the conformation of the nanoactuator device to the S2 state. The mismatched base pairs (in pink) are included in the stem-loop of S1 to avoid the formation of an unwanted kinetically trapped cruciform junction, a possible secondary structure to the S2 state of the nanoactuator device.

The nanoactuator designed here differs significantly from a conventional molecular beacon[10] in that the nanoactuator has a well-defined conformation that can be easily incorporated into DNA lattices, the motion generated is translated along a stacked double helix, and the reversible interconversion between states is executed through strand displacement using a DNA fuel strand. Yurke and Turberfield[5] first introduced strand displacement by using a fuel strand for the construction of a DNA tweezer that executes an open/close motion. We utilize this technique to interconvert the nanoactuator device described here. Both the set strands in the device have a 3′ extension of eight nucleotides, which are used as a handle to initiate branch migration upon addition of their fuel strands, leading to their removal from the nanoactuator device. Since the set strands and their corresponding fuel strands (FS1 and FS2) are complementary along their entire length, pairing of a set strand and its fuel strand is energetically more favored than partial pairing of the set strands in the S1 and S2 state. Both fuel strands have a biotin group at their 5′-ends indicated in Figure 1 by a filled black circle. The waste product composed of the complementary duplex of set strand and fuel strand can be removed, if desired, by treatment with streptavidin magnetic-bead separation. The nanoactuator device operates as follows: starting from S1, SS1 (red) is removed by the addition of FS1 (green), producing the unpaired intermediate (INT), which is then fixed to S2 by the addition of SS2 (blue). Addition of FS2 (purple) to remove SS2 converts S2 to the unpaired intermediate (INT). Addition of a SS1 (red) restores the S1 state and completes the cycle. Operation of the nanoactuator device will result in an extension/contraction motion of two turns of DNA (~6.8 nm) along the stacked helix.

We used both gel electrophoresis and fluorescent resonance energy transfer spectroscopy (FRET) to demonstrate the interconversion and cycling of the nanoactuator device. In Figure 2a the electrophoresis with 14% nondenaturing polyacrylamide gel shows the formation and operation of the device. Lane LM contains 50-base-pair (bp) DNA linear

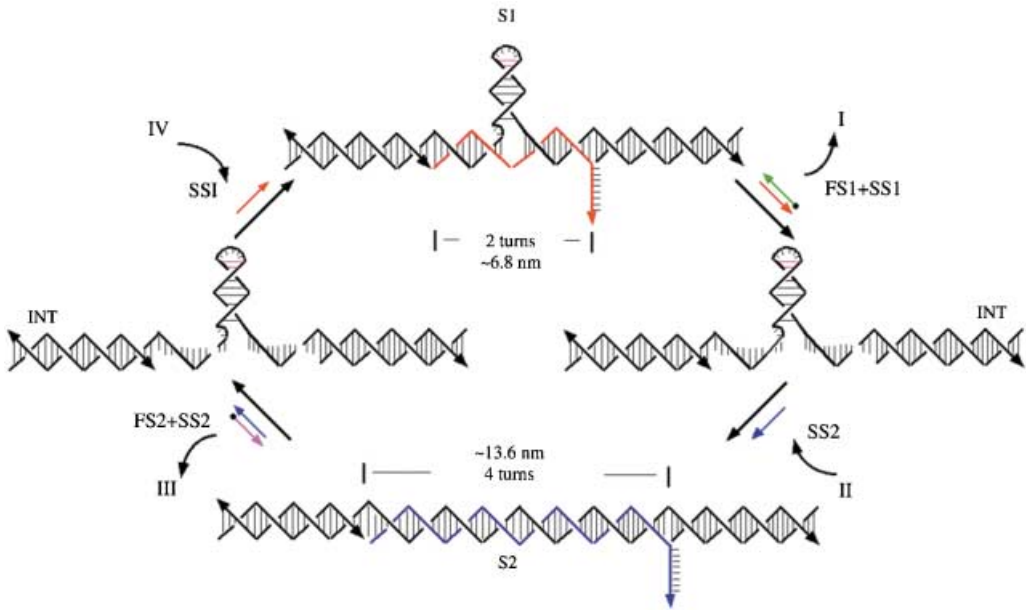

Figure 1. Schematic drawing of the design and operation of the nanoactuator device. I-IV represent the four steps to complete one cycle of the device operation. See the text for an explanation.

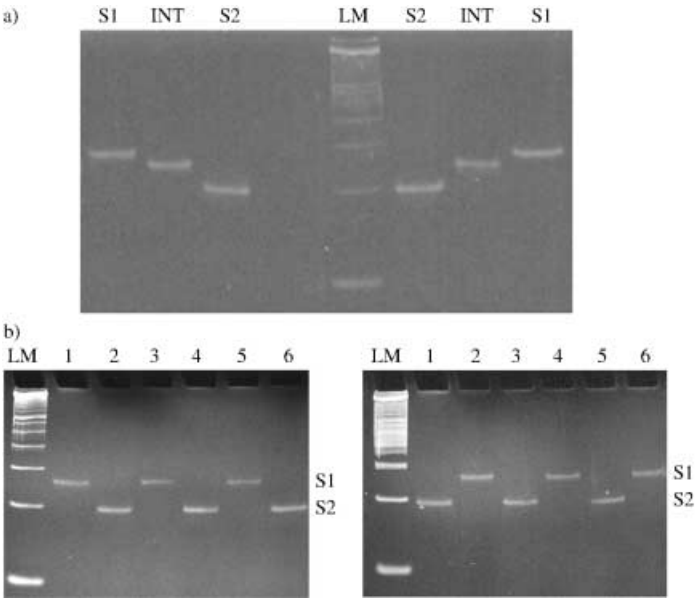

Figure 2. Gel evidence for the cycling of the nanoactuator device. See text for an explanation.

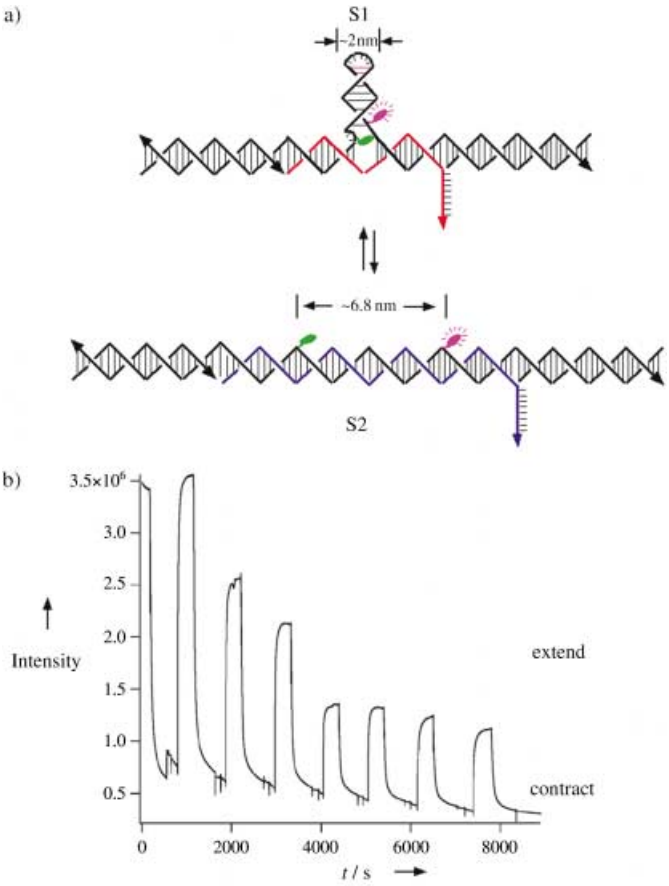

Figure 3. FRET measurements for the cycling of the nanoactuator device. a) Schematic drawing of the incorporation of fluorescent dyes in the nanoactuator device. A donor, fluorescein, and an acceptor, Tamra,are represented as green and purple filled circles, respectively. b) Cycling the nanoactuator device measured by FRET spectroscopy.

markers. The operation was demonstrated starting either from S1 (left side of the marker lane) or from S2 (right side of the marker lane). The linear duplex of S2 migrates faster than the bulged-junction of S1 although its molecular weight is greater than that of S1. An intermediate species (labeled as INT) appears as single band between S1 and S2, indicating the robustness of the nanoactuator during the process of switching. Figure 2b shows electrophoresis images with nondenaturing gel demonstrating the interconversion between the two states of the nanoactuator device in three cycles, starting with S1 (left panel) and S2 (right panel). Lane 1 is the initial conformation (S1 at left panel and S2 at right panel), and lanes 2 to 6 show alternating transformations to the other state. Cycling of the nanoactuator device was achieved by alternatively adding an equal molar ratio of the fuel strand and the set strand as illustrated in Figure 1, and the waste products were removed by streptavidin magnetic-bead treatment. The absence of species other than the molecules in the S1 or S2 state of the nanoactuator device attests to the robustness of the device in bulk. It also confirms that the design of including mismatched bases in the stem-loop prevents the formation of any unwanted secondary structure. To make sure the transition of the DNA nanoactuator results from structural transformation, we also engineered a restriction site in the device and demonstrated the conformational change between the two states of the nanoactuator (see Supporting Information).

FRET is a valuable method to obtain information on the structure of nucleic acids because of its distance and orientation dependence. As illustrated in Figure 3, two fluorescent dyes—a donor, fluorescein, and an acceptor, Tamra,—are covalently bound to the backbone of the long black strand at the positions of the turns of the junction. The distance between the two dyes is expected to increase upon transition from S1 to S2. Thus the efficiency of the FRET would decrease, causing the light up of the donor upon formation of S2 state. Figure 3b shows interconversion of the nanoactuator device in seven cycles. The extension and contraction of the nanoactuator device is fully reversible and the switching time for the machine is 26 ± 2 s. The interconversion of the nanoactuator device was achieved by alternatively adding fuel strands and set strands to the solution for each state. The waste products were not removed from the solution in this case. The decrease of the intensity of the FRET signal by almost threefold over the course of the interated switching of the device is due to the dilution of the solution when the fuel and set strands are added to the solution. These results, in addition to the results of gel electrophoresis, clearly indicate that the nanoactuator device described here oscillates between two well-defined states.

To realize potential applications of the DNA nanoactuator device constructed here, the device must be integrated into nanorobotics or patterned arrays so that a functional network of nanoactuator devices can be built. We demonstrated a major step toward this goal by implementing the device constructed here into a 2D DNA lattice, and the state of the lattice can be actuated through the operation of this device. Figure 4 illustrates the design of a such a structure.

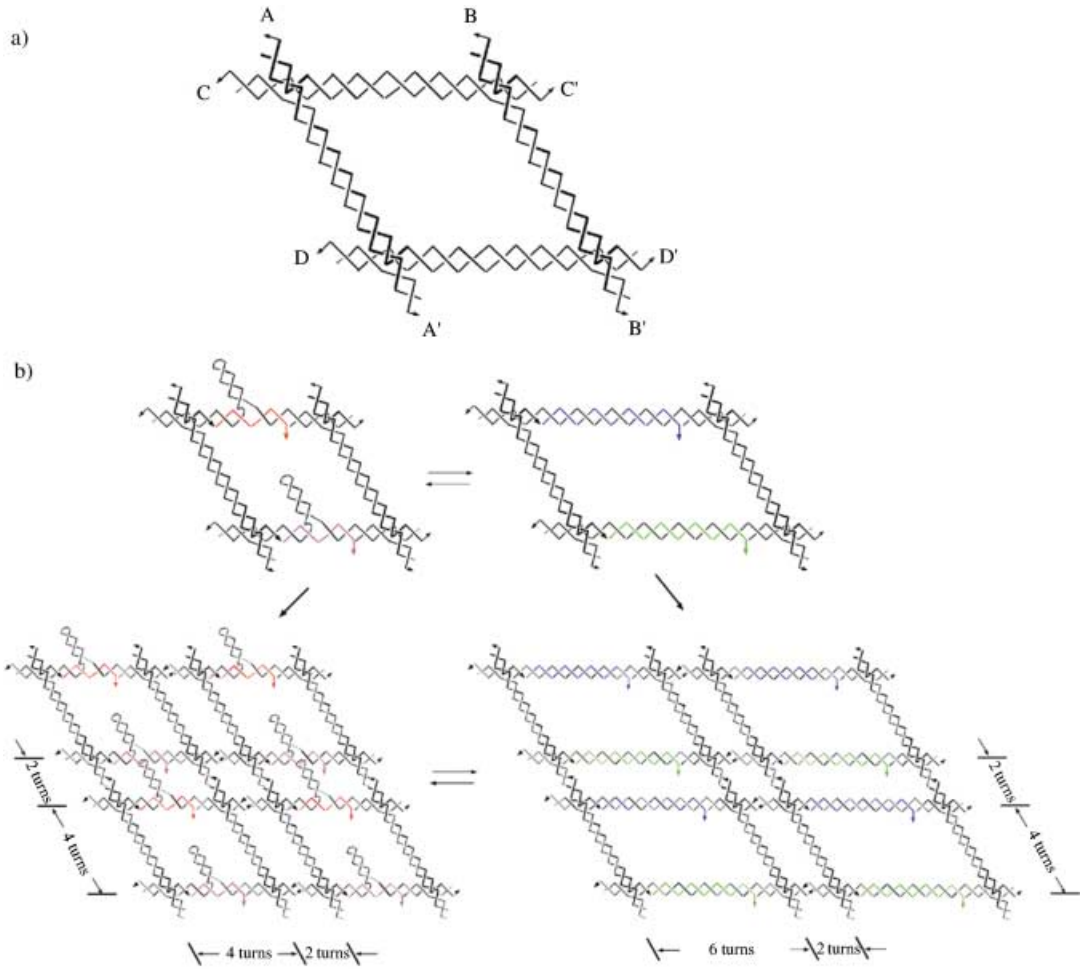

Figure 4. Schematic drawing of the two-state 2D lattices actuated by DNA nanoactuator devices. a) A unit for self-assembly of parallelogram lattice (described in ref. [4]) containing complementary sticky ends, for example, A and A′, which will self-assemble into a 2D lattice. b) Incorporation of DNA nanoactuator devices into 2D lattice. Two nanoactuator devices with different base sequences are incorporated into the opposite arms of the rhombuslike motif. The two states of these nanoactuator devices result in two different lattice components. Sticky-ended association will lead to 2D lattices. Periodicity of the lattice is illustrated by their helical turns.

The nanoactuator device is incorporated into a 2D DNA lattice constructed previously by Mao et al.,[3] which was demonstrated to display a rhombuslike cavity with size of ~14 nm in each of the two dimensions. The unit of the previously demonstrated parallelogram contains four four-arm branched junctions (Figure 4a), which were fused into a rhombuslike molecule. The branch points, which define vertices, are each separated by four double-helical turns. The rhombuses were directed to self-assemble by hydrogen bonding into a two-dimensional periodic array, whose spacing is six turns in each direction. In our design, we modified the molecule and incorporated two nanoactuator devices into two opposite edges of the unit (Figure 4b). The operation of the nanoactuator devices will result in a contraction/extension motion of the 2D lattice assembled from the designed unit, as illustrated in lower panel of Figure 4b.

We performed the interconversion of the nanoactuator device in solution and demonstrated the motion of the lattice by imaging samples deposited on mica using atomic force microscopy (AFM). The AFM images in Figure 5 illustrate

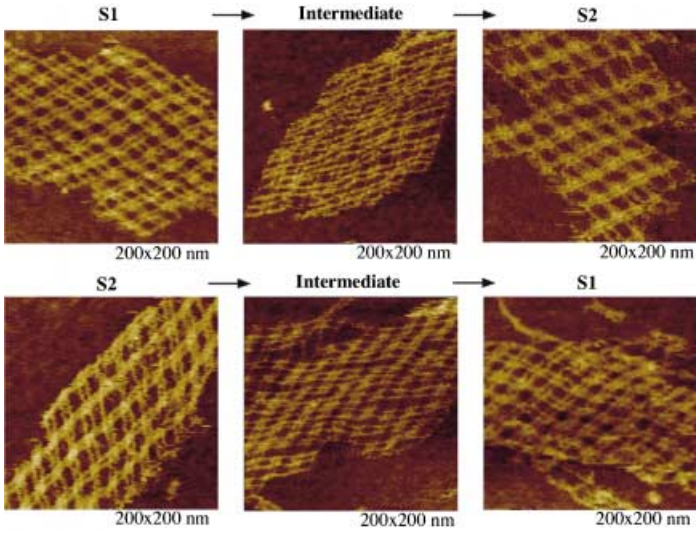

Figure 5. AFM evidence for the two state DNA lattice actuated by DNA nanoactuator devices. For details see text.

the change of the DNA lattices upon the operation of the nanoactuator device. In the upper panel of Figure 5 the three AFM images demonstrate the switching of the nanoactuator device from S1 to the intermediate state and then to S2. A change in the size of the cavity in the lattice was observed after the operation was complete. The dimensions of each rhombus cavity in the lattice change from $\sim 14 \times 14$ nm to $\sim 14 \times 20$ nm after the operation, which is consistent with the parameters in the design. The three images in lower panel of Figure 5 show the switching of the nanoactuator device from S2 to the intermediate state and then to S1. The dimensions of each rhombus cavity change from $\sim 14 \times 20$ nm to $\sim 14 \times 14$ nm. These clearly confirm that the operation of the nanoactuator devices results in a contraction and extension of the lattice. Thus, the DNA nanoactuator device is functioning in a 2D lattice powered by DNA fuel strands. The AFM images of the intermediate state shown in Figure 5 demonstrate that the lattices in the intermediate state are not as regular as those in the S1 and S2 states. However, the lattice in the intermediate state does not fall apart during the transition of the device, which strongly suggests the robustness of the lattice during the operation of the nanoactuator devices.

In summary, we have constructed and incorporated a robust DNA nanoactuator device into 2D DNA lattices. The nanoactuator device constructed here results in a linear translational motion on the lattice. This nanoactuator device can be modified easily to produce both a translational and a rotational motion by adding an odd number of half-turn-long nucleotides in the stem loop. After strand displacement, there would be a 180° rotation around the axis of the stacked helix. A potential use of such a nanoactuator device is to program the assembly of nanoelectronic components. For example, Loweth et al.[12] used complementary DNA as a template to assemble lines of gold nanoparticles by attaching 5-nm- or 10-nm-sized gold nanoparticles to DNA strands. The nanoactuator device can be used to control the relative orientations of nanoparticles. It is possible to change the relative positions of proteins or other large molecules connected to both ends of the nanoactuator device. This capability may facilitate the study of proximity effects in chemical and biological systems. By controlling the space between molecules, the nanoactuator device may find applications in biosensors development.

Experimental Section

All DNA strands used here are listed in the Supplemental Information. DNA strands were synthesized by Integrated DNA Technologies, Inc. (www.idtdna.com) and purified by denaturing gel electrophoresis. The nanoactuator device complex and the DNA lattice were formed by mixing a stoichiometric quantity of each strand designed in the complex or lattice unit at a concentration of 1 μM, as estimated by OD_{260}, in 1 × TAE/Mg buffer (40 mM Tris·HCl, pH 8.0, 20 mM acetic acid, 2 mM EDTA, and 12.5 mM magnesium acetate). The solution was cooled slowly from 90 °C to 20 °C. For nondenaturing gel electrophoresis, the preformed nanoactuator device complex was subjected to the processes of the interconversion described in Figure 1, sampling aliquots were loaded on gel run at 20 °C for 16 h.

For the FRET experiment, fluorescently labeled, longer length DNA oligomer was obtained by ligating shorter synthesized oligomers. A Fluorolog 3 fluorimeter (Jobin-Yvon–Horiba) was utilized to measure the fluorescence emission spectra and the kinetics of the fluorescence intensity changing with time. $\lambda_{ex} = 485$ nm, $\lambda_{em} = 518$ nm; the slit widths were 2.5 nm for both excitation and emission. After the addition of fuel or set strands, solution was mixed within 2 s by rapidly drawing it up a pipette and then releasing it. All measurements were performed at 20 °C. For AFM imaging, a 5-μL sample of the DNA lattice was applied to freshly cleaved mica (Ted Pella, Inc.) as a drop and left to adsorb to the surface for 3 min. Then 30-μL of 1xTAE/Mg buffer was added to the drop on the mica. Imaging was performed in a fluid cell on a Multimode NanoScope IIIa (Digital Instruments) using NP-S tips (Veeco Inc.).

Received: May 6, 2003 [Z51818]

Keywords: DNA structures · DNA · nanostructures · scanning probe microscopy · self-assembly

[1] E. Winfree, F. Liu, L. A. Wenzler, N. C. Seeman, *Nature* **1998**, *394*, 539 – 544.
[2] T. H. LaBean, H. Yan, J. Kopatsch, F. Liu, E. Winfree, J. H. Reif, N. C. Seeman, *J. Am. Chem. Soc.* **2000**, *122*, 1848 – 1860.
[3] C. Mao, W. Sun, N. C. Seeman, *J. Am. Chem. Soc.* **1999**, *121*, 5437 – 5443.
[4] C. Mao, W. Sun, Z. Shen, N. C. Seeman, *Nature* **1999**, *397*, 144 – 146.
[5] A. J. Yurke, A. P. Turberfield, Jr., Mills, F. C. Simmel, J. E. Neumann, *Nature* **2000**, *406*, 605 – 608.
[6] H. Yan, X. Zhang, Z. Shen, N. C. Seeman, *Nature* **2002**, *415*, 62 – 65.
[7] J. Li, W. Tan, *Nano Lett.* **2002**, *2*, 315 – 318.
[8] P. Alberti, J. Mergny, *Proc. Natl. Acad. Sci. USA* **2003**, *100*, 1569 – 1573.
[9] For a review, see: C. Niemeyer, M. Adler, *Angew. Chem.* **2002**, *114*, 3933 – 3937; *Angew. Chem. Int. Ed.* **2002**, *41*, 3779 – 3783.
[10] S. Tyagi, F. R. Kramer, *Nat. Biotechnol.* **1996**, 14, 303 – 308.
[11] I. V. Ouporov, N. B. Leontis, *Biophys. J.* **1995**, 68, 266 – 274.
[12] C. J. Loweth, W. B. Caldwell, X. G. Peng, A. P. Alivisatos, P. G. Schultz, *Angew. Chem.* **1999**, *111*, 1925 – 1929; *Angew. Chem. Int. Ed.* **1999**, *38*, 1808 – 1812.
[13] B. Liu, N. B. Leontis, N. C. Seeman, *Nanobiology* **1994**, 3, 177 – 188.
[14] J. Qi, X. Li, X. P. Yang, N. C. Seeman, *J. Am. Chem. Soc.* **1996**, *118*, 6121 – 6130.
[15] X. J. Li, X. P. Yang, J. Qi, N. C. Seeman, *J. Am. Chem. Soc.* **1996**, *118*, 6131 – 6140.

